

# A plastic strain based statistical damage model for brittle to ductile behaviour of rocks

Changtai Zhou<sup>1,2</sup>, Kai Zhang<sup>\*1,2</sup>, Haibo Wang<sup>3</sup> and Yongxiang Xu<sup>4</sup>

<sup>1</sup>Guangdong Provincial Key Laboratory of Deep Earth Sciences and Geothermal Energy Exploitation and Utilization, Institute of Deep Earth Sciences and Green Energy, College of Civil and Transportation Engineering, Shenzhen University, Shenzhen, China

<sup>2</sup>Shenzhen Key Laboratory of Deep Underground Engineering Sciences and Green Energy, Shenzhen University, Shenzhen, China

<sup>3</sup>Department of Civil Engineering, Nanjing Forestry University, Nanjing, China

<sup>4</sup>Mining Institute, China Coal Research Institute, Beijing, China

(Received August 31, 2019, Revised April 2, 2020, Accepted April 3, 2020)

**Abstract.** Rock brittleness, which is closely related to the failure modes, plays a significant role in the design and construction of many rock engineering applications. However, the brittle-ductile failure transition is mostly ignored by the current statistical damage constitutive model, which may misestimate the failure strength and failure behaviours of intact rock. In this study, a new statistical damage model considering rock brittleness is proposed for brittle to ductile behaviour of rocks using brittleness index (BI). Firstly, the statistical constitutive damage model is reviewed and a new statistical damage model considering failure mode transition is developed by introducing rock brittleness parameter-BI. Then the corresponding damage distribution parameters, shape parameter  $m$  and scale parameter  $F_0$ , are expressed in terms of BI. The shape parameter  $m$  has a positive relationship with BI while the scale parameter  $F_0$  depends on both BI and  $\epsilon_e$ . Finally, the robustness and correctness of the proposed damage model is validated using a set of experimental data with various confining pressure.

**Keywords:** rock brittleness; constitutive model; plastic strain; damage model; deep earth science

## 1. Introduction

A thorough understanding of the strength and deformation behaviours of rock is vital to the design and construction of rock engineering applications including tunnel for deep mining, storage of radioactive waste, wellbore for oil or gas production and excavation for underground space (Xie *et al.* 2020). The complete stress-strain curves of rock under compression provide us an effective way to understand the rock deformation and failure behaviours (Cao *et al.* 2010, Xue 2015), which will facilitate the design and stability of these engineering structures. Therefore, constructing a suitable constitutive model to represent the strength and deformation behaviours is an everlasting concentration for engineering applications (Martin and Chandler 1994, Cao *et al.* 2018).

Complicated mechanical responses such as strain softening, strain hardening and failure modes transition can be observed from these stress-strain curves derived from laboratory scale due to external factors (Wawersik and Fairhurst 1970, Horii and Nemat-Nasser 1986, Evans *et al.* 1990, Fredrich *et al.* 1990, Peng *et al.* 2015, 2017). The confining pressure is the main factor influencing the mechanical responses of rocks, which can lead to the failure mode transition from brittle fracturing to diffuse plastic flow (Peng 1973, Stavrogin and Tarasov 2001, Mas and

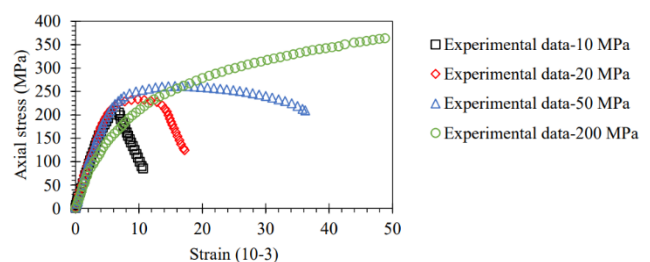


Fig. 1 A transition from brittleness to ductileness of rocks exposed to confining pressure. After Mas and Chemenda (2015)

Chemenda 2015), see Fig. 1. The transition behaviour of rocks may be related to the initiation and propagation of micro-cracks in rocks from a microscopic mechanism perspective (Fuenkajorn *et al.* 2012). At a relatively low confining pressure, those micro-cracks become active at low stress levels, and grow and coalesce to macroscopic fractures, leading to abrupt failures when the critical stress is reached. However, as the confining stress increases, a higher level of stress is achieved before micro-cracks coalescence occurs; thus, a greater number of micro-cracks participate in the failure process, and the failure behaviour becomes increasingly more ductile and diffuse.

To quantify the degree of brittleness/ductility, the concept of brittleness index (BI) was proposed by many researchers (Hucka and Das 1974, Andreev 1995, Holt *et al.* 2015, Akinbinu 2017, Chen *et al.* 2017). However, there is no unique definition of brittleness parameter as stated in previous studies (Hucka and Das 1974, Holt *et al.* 2015,

\*Corresponding author, Ph.D.

E-mail: zhangkai@my.swjtu.edu.cn

Akinbinu 2017). Many methods were proposed to quantify the rock brittleness based on various measurement methods, such as strain characteristics, stress characteristics, rock strength properties, rock mineral constituents, and energy balance methods (Rahimzadeh Kivi *et al.* 2018).

To capture the complex responses of rocks, the statistical damage model (SDM) has been favoured by many researchers due to the easy implementation into computer code and application to engineering analysis (Tang *et al.* 1998, Cao *et al.* 2010, 2018, Deng and Gu 2011, Li *et al.* 2012, Liu and Yuan 2015, Wang *et al.* 2016, Zhou *et al.* 2020). In classical SDM, it is believed that the rock is a type of material with microscopic cracks, and the damage process can be regarded as the process of micro-cracks initiation, propagation and coalescence in a stochastic manner. Thus, the SDM provides us with a venue to investigate the complex responses of rocks. The softening and hardening behaviours of rocks have been explored by Cao *et al.* (2010). In this model, the damage process and mechanical responses of rocks mentioned above were believed associated with the variance of voids or pores in the natural rocks. Additionally, the strain softening behaviours can be reflected by the SDM proposed by Li *et al.* (2012) to a certain degree. Due to the emphasis of their study, it did not develop a strategy for strain softening and strain hardening of rocks. The above-mentioned SDMs based on the statistical damage mechanics have shown their own merits, however, the failure mode transition induced by external factors mentioned above is seldom presented by a constitutive model using the framework of statistical damage mechanics. Therefore, it is still necessary to develop a SDM for rocks to capture the essential mechanical response, like the failure mode transition, using a set of parameters.

Motivated by these previous studies, in this study, we propose a SDM by incorporating *BI* to capture the brittle-ductile transition. The brittleness characteristics of intact rock in previous experimental investigations are demonstrated in the following section. Then, a new damage model is proposed by incorporating the brittleness parameter based on the continuum damage theory and the statistical damage mechanics. Finally, a validation study for the proposed damage model is carried out using a set of laboratory results.

## 2. Brittleness index (*BI*)

As mentioned in Section 1, the brittleness of rocks can be quantified through different methods based on different measurements. In Table 1, we summarize different brittleness parameter definitions based on above-mentioned methods. Amongst these definitions of rock brittleness, the most effective and obvious way to define rock brittleness is using the stress and strain characteristics based on the stress-strain curve, see Fig. 2.

Here we briefly describe the brittleness on the basis of strain-based method and stress-based method, which will be incorporated into the proposed damage model. Hucka and Das (1974) defined brittleness as the ratio of elastic strain  $\varepsilon_e$  to the total strain or failure strain  $\varepsilon_f$  based on the

Table 1 Summary of brittleness definitions in the literature

Methods	Formulation	Comments	References
Strain	$BI_1 = \varepsilon_e / \varepsilon_f$	$\varepsilon_e$ is the total elastic strain, $\varepsilon_f$ is the failure strain; $\varepsilon_r$ is the residual strain;	(Hucka and Das 1974)
	$BI_2 = (\varepsilon_r - \varepsilon_f) / \varepsilon_r$	$\varepsilon_f^p$ is the plastic strain when frictional strength is fully mobilized; plastic strain when cohesive strength is completely degraded.	(Andreev 1995)
	$BI_3 = (\varepsilon_f^p - \varepsilon_c^p) / \varepsilon_c^p$		(Hajiabdolmaji <i>et al.</i> 2002)
Stress	$BI_4 = \sigma_r / \sigma_f$	$\sigma_r$ is the residual strength;	(Andreev 1995)
	$BI_5 = (\sigma_f - \sigma_r) / \sigma_f$	$\sigma_f$ is the failure strength	(Smolczyk and Gartung 1979)
Rock strength	$BI_6 = \sigma_u / \sigma_t$	$\sigma_u$ is the uniaxial compressive strength	(Andreev 1995)
	$BI_7 = (\sigma_u - \sigma_t) / \sigma_u + \sigma_t$	$\sigma_t$ is the tensile strength	(Hucka and Das 1974)
	$BI_8 = \sigma_u * \sigma_t / 2$		(Altindag 2003)
Rock mineral constituents	$BI_9 = F_{sb} / (F_{sb} + F_{wd})$	$F_{sb}$ is the fraction of brittle minerals, $F_{wd}$ is the fraction of ductile minerals.	(Rybacki <i>et al.</i> 2016)
Energy analysis	$BI_{10} = dW_{et} / (dW_{et} + dW_p)$	$W_{et}$ is the total elastic energy, $W_p$ is the plastic energy.	(Hucka and Das 1974)

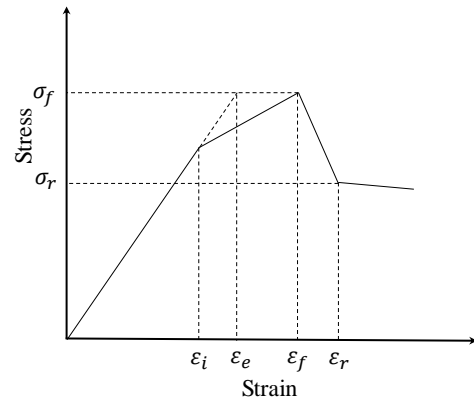


Fig. 2 Typical stress-strain curve of rock material.  $\varepsilon_i$ ,  $\varepsilon_e$ ,  $\varepsilon_f$  and  $\varepsilon_r$  are the strain for the onset of dilatancy, elastic strain, failure strain and residual strain;  $\sigma_f$  and  $\sigma_r$  are failure strength and residual strength (after Rybacki *et al.* 2016)

stress-strain curve:

$$BI_1 = \varepsilon_e / \varepsilon_f \quad (1)$$

where  $\varepsilon_e$  and  $\varepsilon_f$  are elastic and failure strain, respectively. Instead of focusing on the pre-peak failure behaviour, Andreev (1995) used the residual strain  $\varepsilon_r$  and residual stress  $\sigma_r$  to define the brittleness index:

$$BI_2 = (\varepsilon_r - \varepsilon_f)/\varepsilon_r \quad (2)$$

$$BI_4 = \sigma_r/\sigma_f \quad (3)$$

where  $\varepsilon_r$  is the residual strain;  $\sigma_r$  and  $\sigma_f$  are residual stress and failure stress, respectively. Smolczyk and Gartung (1979) modified Eq. (3) to the following expression:

$$BI_5 = (\sigma_f - \sigma_r)/\sigma_f \quad (4)$$

In this study, for simplicity, the brittleness using the elastic strain and failure strain, see Eq. (1), is implemented into the statistical damage model to capture the brittleness/ductility mechanical responses.

### 3. The classical statistical damage model (SDM)

In this section, the fundamentals of the classical SDM developed by previous studies are firstly reviewed and presented.

#### 3.1 Damage evolution law

In nature, intact rock contains many microscopic elements such as microscopic cracks and defects. Therefore, the damage process can be regarded as the process of micro-cracks initiation, propagation and coalescence (Cao *et al.* 2010). Assuming the strength of microscopic element is randomly distributed, a SDM can be established based on statistical damage mechanics. Two steps are needed to establish a SDM (Liu and Yuan 2015): choosing a proper failure criterion for micro-cracks, such as the maximum strain criterion, Mohr-Coulomb criterion and Drucker-Prager criterion; and then determining a certain distribution of these micro-cracks such as Power- and Weibull distribution. In this study, the Weibull distribution is adopted for the strength distribution of microscopic elements.

Applying the Weibull distribution to the microscopic strength distribution of microscopic elements, the probability density function is (Weibull 1951):

$$P(F) = \frac{m}{F_0} \left(\frac{F}{F_0}\right)^{m-1} \exp\left[-\left(\frac{F}{F_0}\right)^m\right] \quad (5)$$

where  $F$  is an elemental strength parameter depending on the strength criterion used;  $m$  is the shape parameter or a homogeneous index of Weibull distribution;  $F_0$  is the scale parameter of Weibull distribution.

Adopting the maximum strain theory (Tang *et al.* 1998) as the failure criterion of microscopic element strength,  $F$  can be replaced by the strain  $\varepsilon$ . Then the probability density function becomes:

$$P(\varepsilon) = \frac{m}{F_0} \left(\frac{\varepsilon}{F_0}\right)^{m-1} \exp\left[-\left(\frac{\varepsilon}{F_0}\right)^m\right] \quad (6)$$

Assuming the total number of microscopic elements is  $N$  and the number of failed microscopic elements is  $n$ , we define the damage variable  $D$  as the ratio of the number of failed elements to the total microscopic elements:

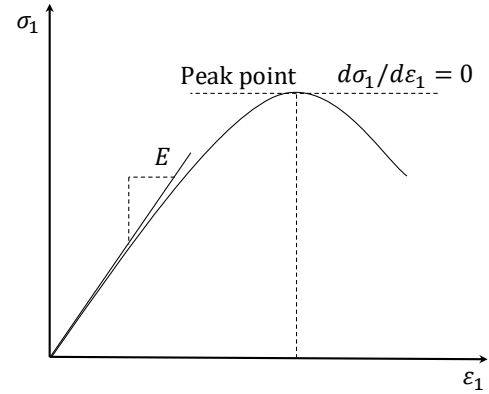


Fig. 3 Determination of damage distribution parameters using the Extremum method. After Li *et al.* (2012)

$$D = \frac{n}{N} \quad (7)$$

where damage variable  $D$  falls in the range between 0 and 1. If local strain increases from 0 to  $F$ , the number of failed microscopic elements  $n$  is:

$$n = N \int_0^F P(\varepsilon) dF = N \left\{ 1 - \exp\left[-\left(\frac{\varepsilon}{F_0}\right)^m\right] \right\} \quad (8)$$

Substituting Eq. (8) into Eq. (7), the damage variable can be expressed:

$$D = 1 - \exp\left[-\left(\frac{\varepsilon}{F_0}\right)^m\right] \quad (9)$$

Assuming the stress acting on the effective area of the damaged material is the effective stress  $\sigma_{ij}^*$ , based on the Lemaitre's strain-equivalent principle (Lemaitre 1984), the effective stress  $\sigma_{ij}^*$  can be expressed using nominal stress  $\sigma_{ij}$ :

$$\sigma_{ij}^* = \sigma_{ij}/(1 - D) \quad (10)$$

According to the generalized Hooke's law, the strain can be expressed in the following equation on the principal stress direction:

$$\varepsilon_i = \frac{1}{E} [\sigma_i^* - \mu(\sigma_j^* + \sigma_k^*)] \quad (11)$$

where  $\mu$  is the Poisson's ratio. Substituting Eq. (10) into Eq. (11), one can obtain the stress-strain relationship:

$$\varepsilon_i = \frac{1}{E(1 - D)} [\sigma_i - \mu(\sigma_j + \sigma_k)] \quad (12)$$

Then the stress-strain relationship is obtained on the major principal stress direction:

$$\sigma_i = E\varepsilon_i \exp\left[-\left(\frac{\varepsilon_i}{F_0}\right)^m\right] + \mu(\sigma_j + \sigma_k) \quad (13)$$

#### 3.2 Determination of damage parameters $m$ and $F_0$

In the SDM, two Weibull distribution parameters ( $m$  and  $F_0$ ) can be determined through 'Extremum method' (Cao *et al.* 2010, Deng and Gu 2011). In the stress-strain curve, the

peak point is quite close to the yield point which can be used to determine the model parameters  $m$  and  $F_0$ . At the peak point, the derivative of  $\sigma_1$  with corresponding  $\varepsilon_1$  should be zero, see, Fig. 3, i.e.,:

$$\varepsilon_1 = \varepsilon_{1f}, \sigma_1 = \sigma_{1f} \quad (14)$$

$$\varepsilon_1 = \varepsilon_{1f}, \frac{d\sigma_1}{d\varepsilon_1} = 0 \quad (15)$$

where  $\sigma_{1f}$  and  $\varepsilon_{1f}$  are stress and strain corresponding to the peak point. Substituting (14) and (15) into differentiated Eq. (13), the distribution parameter  $m$  and  $F_0$  can be calculated through the following equations:

$$m = \frac{1}{\ln\{E\varepsilon_{1f}/[\sigma_{1f} - \mu(\sigma_2 + \sigma_3)]\}} \quad (16)$$

$$F_0 = \sqrt[m]{m}\varepsilon_{1f} \quad (17)$$

### 3.3 Incorporating rock brittleness index-BI

To derive the rock response of intact rock, the damage distribution parameters can be calculated with determined failure strength, failure strain and Young's modulus of intact rock, which can be obtained through laboratory tests. However, it is hard to determine the failure strain of rocks, and Li *et al.* (2012) suggested to obtain the failure strain through the laboratory tests. Based on the definition of strain-based brittleness, the failure strain can be determined through Eq. (1) with determined Young's modulus and  $BI$ .

A variety of  $BI$  definitions have been proposed to obtain the rock brittleness as stated in Section 2. Invoking Eq. (1) and introducing the plastic strain, the rock brittleness can be expressed:

$$BI = \frac{\varepsilon_e}{\varepsilon_e + \varepsilon_p} = \frac{\varepsilon_e}{\varepsilon_{1f}} \quad (18)$$

where  $\varepsilon_e$  and  $\varepsilon_p$  are the elastic and plastic strain, respectively, and  $\varepsilon_e + \varepsilon_p$  equals to the total failure strain  $\varepsilon_{1f}$  on the major principal stress direction. Then the damage distribution parameter  $m$  becomes:

$$m = \frac{1}{\ln\{E\varepsilon_{1f}/[\sigma_{1f} - \mu(\sigma_2 + \sigma_3)]\}} = \frac{1}{\ln\{\sigma_{1f}/BI[\sigma_{1f} - \mu(\sigma_2 + \sigma_3)]\}} \quad (19)$$

From the expression of damage distribution parameter  $m$ , we can conclude that it is independent of the failure strength and deformation modulus and is only related to the rock brittleness parameter. The damage distribution parameter  $F_0$  becomes:

$$F_0 = \sqrt[m]{m} \frac{\varepsilon_e}{BI} = \sqrt[m]{m} \frac{\sigma_{1f}}{E * BI} \quad (20)$$

Then the stress-strain relationship on the principal stress direction becomes:

$$\sigma_1 = E\varepsilon_1 \exp \left[ \left( \frac{E * BI}{\sqrt[m]{m} * \sigma_{1f}} \varepsilon_1 \right)^{\frac{1}{\ln\{\sigma_{1f}/BI[\sigma_{1f} - \mu(\sigma_2 + \sigma_3)]\}}} \right] + \mu(\sigma_2 + \sigma_3) \quad (21)$$

## 4. Model validation

To assess the capability of the proposed damage model in predicting the brittleness/ductility responses on rocks, the experimental results mentioned in Section 1 with various confining pressure are compared with the theoretical predictions derived from our proposed damage model i.e. Eq. (21). In this section, the model parameters determination process is first presented and then we discuss the comparison between experimental and theoretical results.

The following steps are used to derive the damage distribution parameters, damage variable and corresponding stress-strain curves (see Fig. 4).

- (1) Identify the basic material parameters including brittleness parameter  $BI$ , failure strength  $\sigma_{1f}$  and Young's modulus  $E$  or elastic strain  $\varepsilon_e$  based on the experimental results;
- (2) Calculate the damage distribution parameters  $m$  and  $F_0$  through Eqs. (19) and (20), respectively;
- (3) Derive the damage variable  $D$  expression from Eq. (9);
- (4) Substitute damage distribution parameters  $m$  and  $F_0$  into Eq. (21) to obtain the rock response.

The experimental results from Mas and Chemenda (2015) on Tavel limestone under the confining pressure of 10, 20, 50 and 200 MPa are considered for validation. From the experimental results, as the confining stress increases from 10 MPa to 200 MPa, a clear transition from brittle failure behaviours, strain-softening to strain hardening behaviours is observed. Following the implementation procedure mentioned in Section 4.1, the damage parameters were calculated from the presented results and summarized in Table 2.

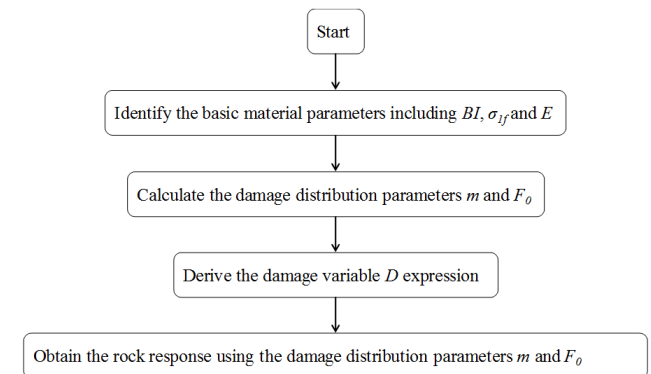


Fig. 4 Flow chart of the implementation of the proposed damage model

Table 2 Damage parameters for the Tavel Limestone with various confining pressure

Confining pressure (MPa)	$BI$	$m$	$F_0$
10	0.76	3.64	392.51
20	0.55	1.67	576.22
50	0.35	0.95	710.21
200	0.13	0.49	653.56

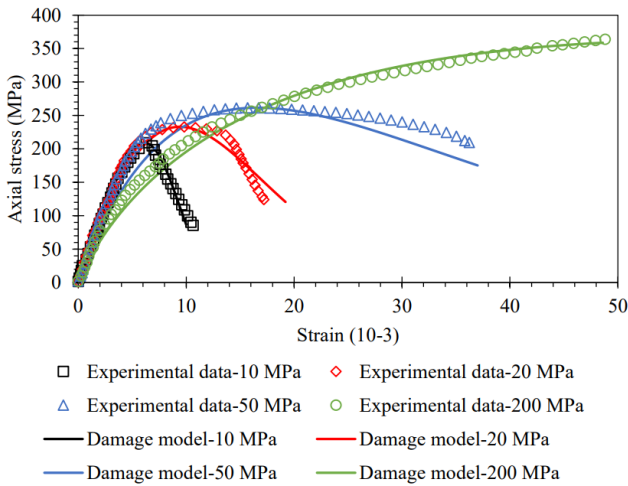


Fig. 5 Comparison between the proposed damage model and experimental results (Mas and Chemenda 2015) under various confining stress

It indicates that the  $BI$  negatively relates to the confining pressure. Then the corresponding damage parameters including the shape parameter  $m$  and the scale parameter  $F_0$  are calculated through Eqs. (19) and (20), respectively, and listed in Table 2. The shape parameter  $m$  decreases from 3.64 to 0.49 as the confining pressure increases, showing a similar tendency as  $BI$ . On the other hand, the scale parameter increases from 392.51 to 710.22 firstly as the confining pressure increases from 10 MPa to 50 MPa, however, decreases to 653.56 when the confining pressure increases up to 200 MPa. It may lie in that the scale parameter depends on a set of factors including  $BI$ ,  $\sigma_{1f}$  and  $E$ .

Based on the derived damage parameters and  $BI$ , the corresponding stress-strain curves for Tavel limestone can be derived, as plotted in Fig. 5 together with experimental results.

The theoretical results obtained from our proposed model are in good agreement with the experimental results. Therefore, the proposed statistical damage model can predict the main experimental results both pre- and post-peak failure behaviours, and correctly capture the brittle/ductile mechanical behaviours, including the failure strength, brittle behaviour, strain-softening behaviour, strain hardening behaviour and failure mode as the confining pressure increases.

## 5. Discussion

### 5.1 Sensitivity analysis

In the derived SDM, the damage distribution parameters including the shape parameter  $m$  and the scale parameter  $F_0$  and intact rock response are brittleness parameter  $BI$  related. The influence of  $BI$  on damage distribution parameters and rock response is investigated in this section.

As stated in the previous section, the damage distribution parameter  $m$  only relates to the brittleness

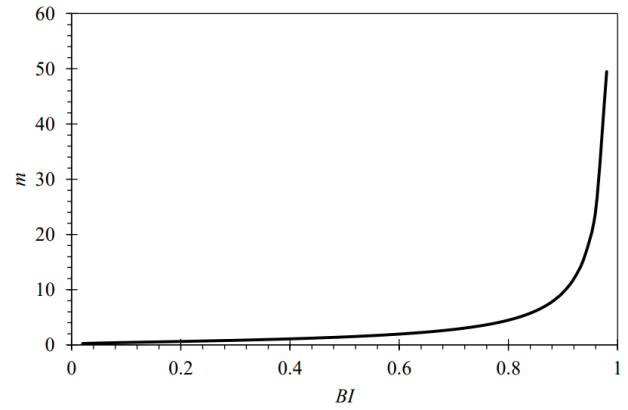


Fig. 6 Damage distribution parameter  $m$  versus rock brittleness parameter  $BI$

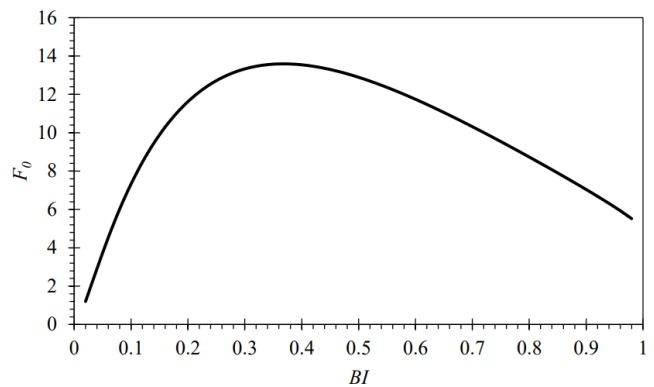


Fig. 7 Damage distribution parameter  $F_0$  versus rock brittleness parameter  $BI$

Table 3 The damage distribution parameters  $m$  and  $F_0$  with corresponding brittleness  $BI$

$BI$	$m$	$F_0$
0.40	1.09	162.51
0.60	1.96	140.91
0.80	4.48	104.81

parameter  $BI$ , indicating that  $m$  reflects the brittleness of the rocks. The relationship between these two parameters is plotted in Fig. 6 from Eq. (19). The shape parameter is nonlinearly and positively related to the brittleness parameter  $BI$ , which confirms the conclusion by previous studies (Liu *et al.* 2017).

The scale parameter  $F_0$  is also plotted against the rock brittleness parameter  $BI$ , where the elastic strain is set to 5 mm, see Fig. 7. The result shows that there is a Parabola relationship between the scale parameter  $F_0$  and the brittleness parameter  $BI$ . The  $F_0$  increases at the initial stage, reaches to the maximum value when  $BI$  equals to 0.36 and then decreases to 5 mm as  $BI$  approaches 1.

To investigate the effect of  $BI$  on the rock response, the failure strength and elastic strain are set to 60.00 MPa and 5.00 mm, respectively, while the brittleness parameter  $BI$  increases from 0.40 to 0.80. The corresponding damage distribution parameters  $m$  and  $F_0$  are listed in Table 3. As the brittleness  $BI$  increases from 0.40 to 0.80, the damage variable  $D$ , damage evolution rate  $D_r$  and stress-strain

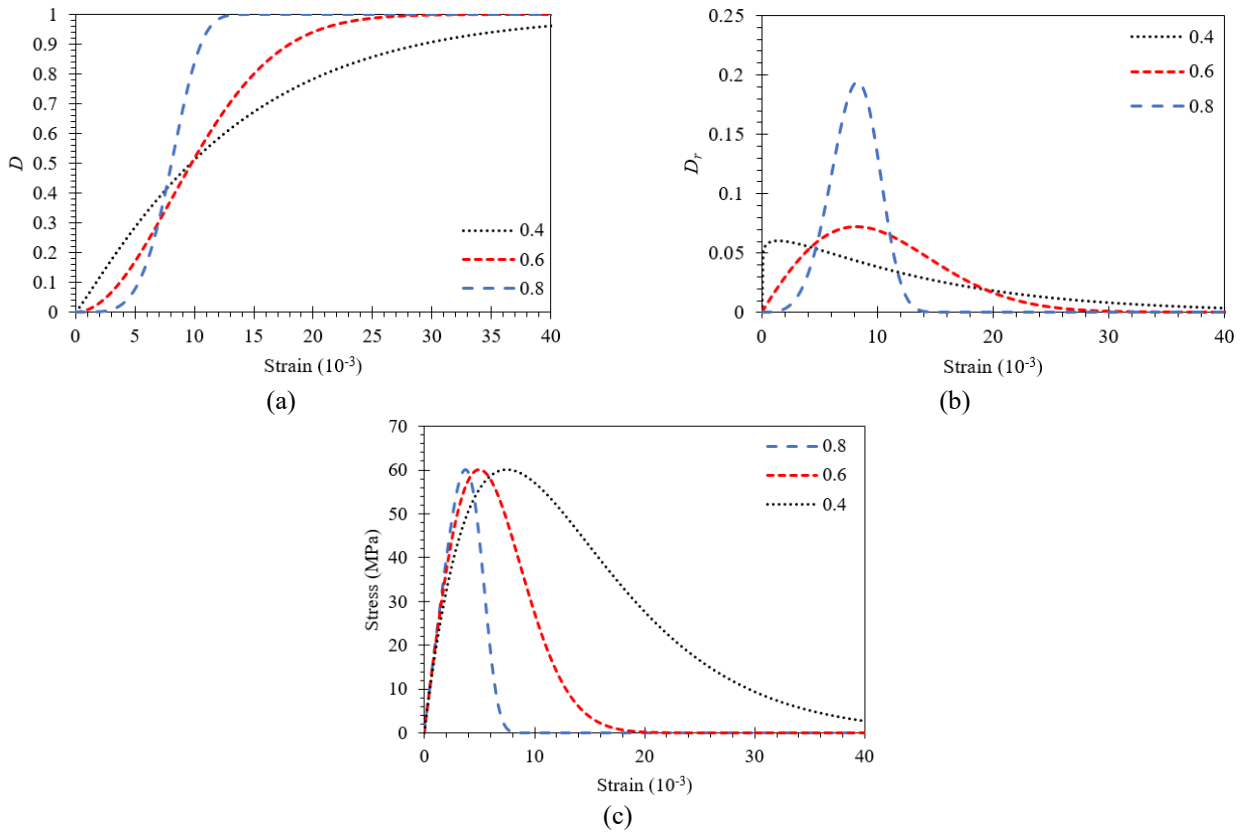


Fig. 8 Damage variable  $D$  (a) Damage evolution rate  $D_r$ , (b) and Intact rock responses and (c) versus the strain with various brittleness parameter  $BI$

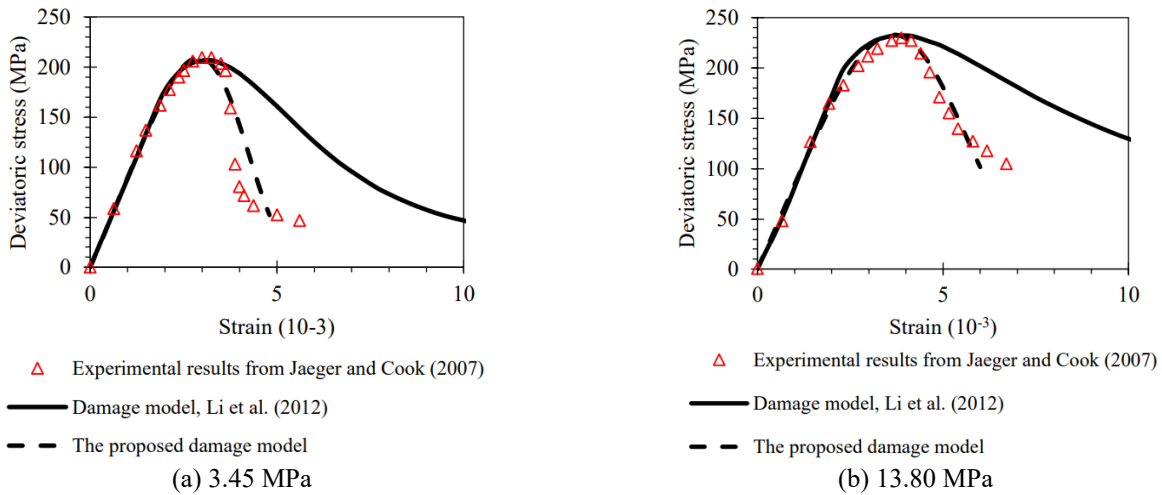


Fig. 9 Comparison between experimental results and theoretical results from previous damage model (Li *et al.* 2012) and the proposed damage model at various confining pressures

relation are plotted Fig. 8, respectively.

As shown in Fig. 8(a), the damage variable  $D$  curve is influenced by the brittleness parameter  $BI$ . As brittleness parameter  $BI$  increases, the damage variable-strain relation becomes steeper, and the strain needed for the onset of damage dramatically increases. The damage evolution increases gradually when  $BI$  is small, i.e.,  $BI=0.40$ . On the other hand, the damage evolution increases quickly when the brittleness parameter  $BI$  is large, i.e.,  $BI=0.80$ . Consequently, the strain needed for the full damage, where

$D=1.00$ , decreases as  $BI$  increases. Overall, the damage model with larger  $BI$  demonstrates more homogeneity characteristics.

In Fig. 8(b), we demonstrate the damage evolution rate  $D_r$  with various brittleness parameter versus strain. As  $BI$  increases, the strain at the maximum damage evolution rate  $D_r$  decreases, which coincide with the dramatic increase in the strain of damage evolution.

The intact rock responses, stress-strain curves, with various  $BI$ , are presented in Fig. 8(c). The results

demonstrate that the peak strength of the damage models is independent of  $BI$ . Additionally, Young's modulus of damage models is also independent of  $BI$  and only depends on the elastic strain. As the brittleness parameter  $BI$  increases, the percentage of the plastic strain out of the total strain is increased. We can conclude that the damage model becomes more ductile as the brittleness parameter  $BI$  decreases. When the brittleness parameter  $BI$  is small, the damage model can tolerate a large inelastic deformation without losing the load-carrying capacity, this is in agreement with previous work (Hajiabdolmajid and Kaiser 2002).

### 5.2 Comparison with the previous damage model

As stated in Section 1, a SDM proposed by (Li *et al.* 2012) to deal with strain softening behaviours for intact rocks. To better evaluate the proposed damage model in this study, the experimental data used for validation in the previous work (Li *et al.* 2012), and theoretical predictions from the previous damage model and the proposed damage model in this study are plotted in Fig. 9 for comparison.

The results showed that theoretical predictions from both damage models have a good agreement with experimental results in terms of pre-peak failure behaviours. However, a clear discrepancy between theoretical prediction based on Li's model and experimental results is observed in the post-peak region. They argued the reason behind this may relate to the failure modes, which can be captured by the proposed damage model in this study. However, our proposed damage model can better capture the post-peak failure behaviours under different confining pressure with less discrepancy. In our damage model,  $BI$  equals to 0.80 and 0.75 with corresponding confining stress of 3.45 and 13.80 MPa. The proposed damage model can better capture the brittle post-failure behaviour compared with Li's damage model.

## 6. Conclusions

As a fundamental problem in rock engineering, rock brittleness is an important property of rocks and is concerned with both pre- and post- peak failure behaviours. In the framework of statistical damage mechanics, we developed a plastic strain based SDM by incorporating the brittleness index ( $BI$ ) to capture the transition from brittle fracture to ductile flow.

The proposed damage model only contains three macroscopic parameters, namely  $BI$ ,  $E$  and  $\sigma_{1f}$ , which can be derived from experimental data. The comparison between theoretical predictions from the proposed damage model and experimental results under various confining pressure indicates that the proposed damage model is able to capture the transition from brittle fracture to ductile flow. The shape parameter  $m$  only relates nonlinearly to the brittleness index ( $BI$ ) of the rocks. However, the scale parameter  $F_0$ , which can be regarded as a strength parameter, depends on both the brittleness parameter- $BI$  and the failure strength adopted.

In further works, the crack closure effect on the mechanical behaviours of rocks at the initial stage should be

taken into consideration to derive a complete stress-strain relation. It may also be more realistic and perhaps more robust for damage models to incorporate stochastic properties of rocks because of the existence of inherent heterogeneity in nature.

## Acknowledgments

The PhD scholarship provided by the China Scholarship Council (CSC) to the first author is gratefully acknowledged. This research is financially supported by the Department of Science and Technology of Guangdong Province (No. 2019ZT08G315) and the Natural Science Foundation of China (No. 51827901).

## References

- Akinbinu, V.A. (2017), "Relationship of brittleness and fragmentation in brittle compression", *Eng. Geol.*, **221**, 82-90. <https://doi.org/10.1016/j.enggeo.2017.02.029>.
- Altindag, R. (2003), "Correlation of specific energy with rock brittleness concepts on rock cutting", *South Afr. Inst. Min. Metall.*, **103**(3), 163-171.
- Andreev, G.E. (1995), *Brittle Failure of Rock Materials*, CRC Press
- Cao, W.G., Zhao, H., Li, X. and Zhang, Y.J. (2010), "Statistical damage model with strain softening and hardening for rocks under the influence of voids and volume changes", *Can. Geotech. J.*, **47**(8), 857-871. <https://doi.org/10.1139/T09-148>.
- Cao, W., Tan, X., Zhang, C. and He, M. (2018), "A constitutive model to simulate the full deformation and failure process for rocks considering initial compression and residual strength behaviors", *Can. Geotech. J.*, **56**(5), 649-661. <https://doi.org/10.1139/cgj-2018-0178>.
- Chen, G., Li, T., Wang, W., Guo, F. and Yin, H. (2017), "Characterization of the brittleness of hard rock at different temperatures using uniaxial compression tests", *Geomech. Eng.*, **13**(1), 63-77. <https://doi.org/10.12989/gae.2017.13.1.063>.
- Deng, J. and Gu, D. (2011), "On a statistical damage constitutive model for rock materials", *Comput. Geosci.*, **37**(2), 122-128. <https://doi.org/10.1016/j.cageo.2010.05.018>.
- Evans, B., Fredrich, J.T. and Wong, T. (1990), *The Brittle-Ductile Transition in Rocks: Recent Experimental and Theoretical Progress*, American Geophysical Union, U.S.A.
- Fredrich, J.T., Evans, B. and Wong, T.F. (1990), "Effect of grain size on brittle and semibrittle strength: Implications for micromechanical modelling of failure in compression", *J. Geophys. Res. Solid Earth*, **95**(B7), 10907-10920. <https://doi.org/10.1029/JB095iB07p10907>.
- Fuenkajorn, K., Sriapai, T. and Samsri, P. (2012), "Effects of loading rate on strength and deformability of Maha Sarakham salt", *Eng. Geol.*, **135-136**, 10-23. <https://doi.org/10.1016/j.enggeo.2012.02.012>.
- Hajiabdolmajid, V. and Kaiser, P. (2002), "Brittleness of rock and stability assessment in hard rock tunneling", *Tunn. Undergr. Sp. Technol.*, **18**(1), 35-48. [https://doi.org/10.1016/S0886-7798\(02\)00100-1](https://doi.org/10.1016/S0886-7798(02)00100-1).
- Hajiabdolmajid, V., Kaiser, P.K. and Martin, C.D. (2002), "Modelling brittle failure of rock", *Int. J. Rock Mech. Min. Sci.*, **39**(6), 731-741. [https://doi.org/10.1016/S1365-1609\(02\)00051-5](https://doi.org/10.1016/S1365-1609(02)00051-5).
- Holt, R.M., Fjær, E., Stenebråten, J.F. and Nes, O.M. (2015), "Brittleness of shales: Relevance to borehole collapse and hydraulic fracturing", *J. Petrol. Sci. Eng.*, **131**, 200-209. <https://doi.org/10.1016/j.petrol.2015.04.006>.

- Horii, H. and Nemat-Nasser, S. (1986), "Brittle failure in compression: splitting, faulting and brittle-ductile transition", *Philos. Trans. R Soc. London Ser A Math Phys. Eng. Sci.*, **319**(1549), 337-374. <https://doi.org/10.1098/rsta.1986.0101>.
- Hucka, V. and Das, B. (1974), "Brittleness determination of rocks by different methods", *Int. J. Rock Mech. Min. Sci.*, **11**(10), 389-392. [https://doi.org/10.1016/0148-9062\(74\)91109-7](https://doi.org/10.1016/0148-9062(74)91109-7).
- Kivi, I.R., Ameri, M. and Molladavoodi, H. (2018), "Shale brittleness evaluation based on energy balance analysis of stress-strain curves", *J. Petrol. Sci. Eng.*, **167**, 1-19. <https://doi.org/10.1016/j.petrol.2018.03.061>.
- Lemaitre, J. (1984), "How to use damage mechanics", *Nucl. Eng. Des.*, **80**(2), 233-245. [https://doi.org/10.1016/0029-5493\(84\)90169-9](https://doi.org/10.1016/0029-5493(84)90169-9).
- Li, X., Cao, W.N. and Su, Y. (2012), "A statistical damage constitutive model for softening behavior of rocks", *Eng. Geol.*, **143-144**, 1-17. <https://doi.org/10.1016/j.enggeo.2012.05.005>.
- Liu, D., He, M. and Cai, M. (2017), "A damage model for modeling the complete stress-strain relations of brittle rocks under uniaxial compression", *Int. J. Damage Mech.*, **27**(7), 1000-1019. <https://doi.org/10.1177/1056789517720804>.
- Liu, H. and Yuan, X. (2015), "A damage constitutive model for rock mass with persistent joints considering joint shear strength", *Can. Geotech. J.*, **52**(8), 1136-1143. <https://doi.org/10.1139/cgj-2014-0252>.
- Martin, C.D. and Chandler, N.A. (1994), "The progressive fracture of Lac du Bonnet granite", *Int. J. Rock Mech. Min. Sci.*, **31**(6), 643-659. [https://doi.org/10.1016/0148-9062\(94\)90005-1](https://doi.org/10.1016/0148-9062(94)90005-1).
- Mas, D. and Chemenda, A.I. (2015), "An experimentally constrained constitutive model for geomaterials with simple friction-dilatancy relation in brittle to ductile domains", *Int. J. Rock Mech. Min. Sci.*, **77**, 257-264. <https://doi.org/10.1016/j.ijrmms.2015.04.013>.
- Peng, J., Cai, M., Rong, G., Yao, M.D., Jiang, Q.H. and Zhou, C. (2017), "Determination of confinement and plastic strain dependent post-peak strength of intact rocks", *Eng. Geol.*, **218**, 187-196. <https://doi.org/10.1016/j.enggeo.2017.01.018>.
- Peng, J., Rong, G., Cai, M. and Zhou, C.B. (2015), "A model for characterizing crack closure effect of rocks", *Eng. Geol.*, **189**, 48-57. <https://doi.org/10.1016/j.enggeo.2015.02.004>.
- Peng, S.S. (1973), "Time-dependent aspects of rock behavior as measured by a servocontrolled hydraulic testing machine", *Int. J. Rock Mech. Min. Sci. Geomech. Abstr.*, **10**(3), 235-246. [https://doi.org/10.1016/0148-9062\(73\)90033-8](https://doi.org/10.1016/0148-9062(73)90033-8).
- Rybacki, E., Meier, T. and Dresen, G. (2016), "What controls the mechanical properties of shale rocks? - Part II: Brittleness", *J. Petrol. Sci. Eng.*, **144**, 39-58. <https://doi.org/10.1016/j.petrol.2016.02.022>.
- Smolczyk, U. and Gartung, E. (1979), "Geotechnical properties of a soft Keuper sandstone", *Proceedings of the 4th International Society for Rock Mechanics and Rock Engineering Congress*, Montreux, Switzerland, September.
- Stavrogin, A.N. and Tarasov, B.G. (2001), *Experimental Physics and Rock Mechanics*, CRC Press
- Tang, C.A., Yang, W.T., Fu, Y.F. and Xu, X.H. (1998), "A new approach to numerical method of modelling geological processes and rock engineering problems-continuum to discontinuum and linearity to nonlinearity", *Eng. Geol.*, **49**(3-4), 207-214. [https://doi.org/10.1016/S0013-7952\(97\)00051-3](https://doi.org/10.1016/S0013-7952(97)00051-3).
- Wang, H., Li, Y., Li, S., Zhang, Q. and Liu, J. (2016), "An elasto-plastic damage constitutive model for jointed rock mass with an application", *Geomech. Eng.*, **11**(1), 77-94. <https://doi.org/10.12989/gae.2016.11.1.077>.
- Wawersik, W.R. and Fairhurst, C. (1970), "A study of brittle rock fracture in laboratory compression experiments", *Int. J. Rock Mech. Min. Sci.*, **7**(5), 561-575. [https://doi.org/10.1016/0148-9062\(70\)90007-0](https://doi.org/10.1016/0148-9062(70)90007-0).
- Weibull, W. (1951), "A statistical distribution function of wide applicability", *J. Appl. Mech.*, **18**, 293-297.
- Xie, H., Zhu, J., Zhou, T., Zhang, K. and Zhou, C. (2020), "Conceptualization and preliminary study of engineering disturbed rock dynamics", *Geomech. Geophys. Geo-Energy Geo-Resour.*, **6**(2), 1-14. <https://doi.org/10.1007/s40948-020-00157-x>.
- Xue, X. (2015), "Study on relations between porosity and damage in fractured rock mass", *Geomech. Eng.*, **9**(1), 15-24. <https://doi.org/10.12989/gae.2015.9.1.015>.
- Zhou, C., Karakus, M., Xu, C. and Shen, J. (2020), "A new damage model accounting the effect of joint orientation for the jointed rock mass", *Arab. J. Geosci.*, **13**(7), 1-13. <https://doi.org/10.1007/s12517-020-5274-3>.

CC

## List of symbols

$BI$	Brittleness index
$D$	Damage variable
$E$ (GPa)	Young's modulus of rocks
$F$	The element strength parameter depending on the strength criterion used
$F_0$	Scale parameter of Weibull distribution
$K$	Compaction coefficient
$m$	Shape parameter or a homogeneous index of Weibull distribution
$N$	The total number of all microscopic elements
$n$	The number of all failed microscopic elements under a certain loading
$P(F)$	The percentage of damaged one out of the total number of microscopic elements in the rock
$\varepsilon_1$	Strain on the major principal stress direction
$\varepsilon_e$	Elastic strain
$\varepsilon_f$	Failure strain or total strain at failure
$\varepsilon_r$	Residual strain
$\mu$	Poisson's ratio of the material
$\sigma_f$ (MPa)	Failure stress
$\sigma_r$ (MPa)	Residual stress
$\sigma_i$ (MPa)	The nominal stress, $i = 1, 3$
$\sigma_i^*$ (MPa)	The effective stress, $i = 1, 3$